# D4.4. Report on scalability of IX and MD/MCr membranes

## Project Information

| | |
|---|---|
| **Grant Agreement Number** | 958454 |
| **Project Full Title** | Intelligent Water Treatment for water preservation combined with simultaneous energy production and material recovery in energy intensive industries |
| **Project Acronym** | intelWATT |
| **Funding scheme** | IA |
| **Start date of the project** | 1$^{st}$ October 2020 |
| **Duration** | 42 months |
| **Project Coordinator** | Andreas Sapalidis (NCSR) |
| **Project Website** | https://www.intelwatt.eu |

## Deliverable Information

| | |
|---|---|
| **Deliverable n°** | D4.4 |
| **Deliverable title** | Report on scalability of ion exchange and MD/MCr membranes |
| **WP no.** | 4 |
| **WP Leader** | NCSR |
| **Contributing Partners** | THK, CUT |
| **Nature** | Report |
| **Authors** | Iosif Scoullos, Ioannis Tournis (NCSR); (CUT) |
| **Contributors** | Stephan Barbe (THK); Ines Betterman |
| **Reviewers** | Andreas Sapalidis (NCSR) |
| **Contractual Deadline** | 30/09/2021 |
| **Delivery date to EC** | 30/09/2021 |

## Dissemination Level

| | | |
|---|---|---|
| PU | Public | ✓ |
| PP | Restricted to other programme participants (incl. Commission Services) | |
| RE | Restricted to a group specified by the consortium (incl. Commission Services) | |
| CO | Confidential, only for the members of the consortium (incl. Commission Services) | |

## Document Log

| Version | Date | Author | Description of Change |
|---------|------|--------|----------------------|
| V1.0 | 16/09/2021 | Iosif Scoullos | First release |
| V2.0 | 27/09/2021 | Iosif Scoullos | Final draft |
| V3.0 | 28/09/2021 | Andreas Sapalidis | Review of the final draft |
| V4.0 | 30/09/2021 | Andreas Sapalidis | Final document |

# Table of Contents

# List of figures

# List of tables

# Abbreviations

| | |
|---|---|
| ATEC | Acetyl Triethyl Citrate |
| AEX | Anion Exchanger |
| BSA | Bovine Serum Albumin |
| CA | Cellulose Acetate |
| CEX | Cation Exchanger |
| CHO | Cyclohexanone |
| $CO_2e$ | Carbon Dioxide-equivalent |
| CPO | Cyclopentanone |
| Cyrene | Dihydrolevoglucosenone |
| DBP | Dibutyl Phthalate |
| DBS | Dibutyl Sebacate |
| DCMD | Direct Contact Membrane Distillation |
| DEC | Diethyl Carbonate |
| DEP | Diethyl Phthalae |
| DI | Deionized |
| DMAc or DMA | Dimethylacetamide |
| DMF | Dimethylformamide |
| DMSO | Dimethyl Sulfoxide |
| DWCs | Dividing Wall Columns |
| EC | Ethylene Carbonate |
| GBL | γ-butyrolactone |
| HF | Hydrogen Fluoride |
| HFP | Hexafluoropropylene |
| HMPA | Hexamethyl Phosphoramide |
| HPAD | Heat Pump Assisted Distillation |
| HVAC | Heating Ventilation And air conditioning |
| ID | Inner Diameter |
| ILs | Ionic Liquids |
| IX | Ion exchange materials |
| LEP | Liquid Entry Pressure |
| LSP | Citric Acid Impregnated Activated Carbon |

| | |
|---|---|
| MCr | Membrane Crystallization |
| MD | Membrane Distillation |
| MEK | Methyl Ethyl Ketone |
| NIC | Nonimpregnated Activated Carbon |
| NIPS | Non-solvent Induced Phase Separation |
| NMP | N−methyl−2−pyrrolidinone |
| OD | Outer Diameter |
| PBT | Persistent Bioaccumulative Toxic |
| PC | Propylene Carbonate |
| PET | Polyethylene Terephthalate |
| PP | Polypropylene |
| PSF | Polysulfone |
| PTFE | PolyTetraFluoroEthylene (Teflon) |
| PVC-C | Chlorinated Polyvinyl Chloride |
| PVC-U | Polyvinyl Chloride Un-plasticised |
| PVDF | Polyvinylidene Fluoride |
| PVDF-HFP | Poly(vinylidene Fluoride)-co-hexafluoropropylene |
| SACX | Strong Acid Cation Exchange Resins |
| SEM | Scanning Electron Microscopy |
| SIPS | Solvent Induced Phase Separation |
| TBSA | N,N' Tetrabutylsuccindiamide |
| TEC | Triethyl Citrate |
| TEP | Triethyl Phosphate |
| THF | Tetrahydrofuran |
| TMP | Trimethyl Phosphate |
| TMU | Tetramethylurea |
| VDF | Vinylidene Fluoride |
| WCA | Water Contact Angle |

# 1 Executive Summary

This document corresponds to the deliverable No.27 (D4.4) "Report on scalability of ion exchange and MD/MCr membranes" of WP4: Tailor made membrane/membrane modules and ion exchange resin development and upscale.

This report focuses on the preparation of Polyvinylidene fluoride (PVDF) and the more hydrophobic copolymer Poly (vinylidene fluoride hexafluoropropylene) (PVDF-HFP) membranes to be used in MD/MCr process. Their preparation will be based on efficient processes, easy to upscale at industrial level. In the beginning, based on previous knowledge and preliminary studies, the consortium has defined the initial synthesis protocols to enable preparation of the flat sheet and hollow fiber membranes. However, within the course of the project, input from laboratory evaluation will guide the selection, modification and optimization of appropriate protocols for the preparation of these membranes. Furthermore, detailed membranes' morphological characterisation and evaluation of performance will also be conducted.

Regarding membranes preparation, both flat sheet and hollow fibers membranes for membrane distillation (MD) and membrane crystallization (MCr) have been prepared by the phase inversion method.

This report analyses the scaling-up process from the lab scale to the pilot scale, as well as the challenges and the options provided at pilot scale. The implementation of customised ion exchange resins in Case Study 3 is also discussed.

# 2  Introduction

This report analyses the scalability of the production of flat sheet and hollow fiber membranes from the current lab scale towards the pilot scale. The upscaling of the selected membranes implies achieving large production of membranes with consistent quality as the ones obtained and validated at small scale. Lab scale development has the advantage of flexibility and many trial-and-error approaches for selecting the optimal production parameters, while the main challenge at pilot scale is to find a balance between large production rate and quality specifications.

The pilot-scale production of membranes must fulfil a series of requirements, such as specifications of the membranes, cost and waste minimisation for volumes needed for the capacity of the pilot plant (membrane area ~100 m$^2$). In addition, waste handling, as well as the environmental footprint of the production process, has also been taken into account.

Two types of membrane geometries will be fabricated: flat sheet and hollow fiber. The most commonly used membrane configurations are the flat sheet membranes, which can be placed either as spiral wound, or plate and frame modules, with the latter allowing higher flow rates, resulting in increase of the productivity, while the membranes can be replaced more easily. On the contrary, these modules have a low packing density and a poor energy efficiency. Spiral wound modules have the advantage of a higher packing density and have an increased energy efficiency compared to the plate and frame modules. Alternatively, hollow fiber membranes can be used. The packing density can then even be increased up to 9,000 m$^2$/m$^3$. However, these modules are lacking turbulence promoters and hence, mixing is relatively poor and more pronounced thermal boundary layers are formed. These modules also suffer more from fouling, reducing or even blocking the inner diameter of the fibers.

In the case of flat sheet membranes for this project, scaling-up involves the use of a new semi-continuous casting system with a roller, while the hollow fibers can be produced with a small modification of the existing semi-continuous equipment used in lab scale; hence, the transference of parameters to bigger scale is in general more direct.

The scalability report follows the structure presented in Figure 1, including production concept at lab scale and at pilot scale, health and safety considerations and waste handling, capacity study and definition of the product costs.
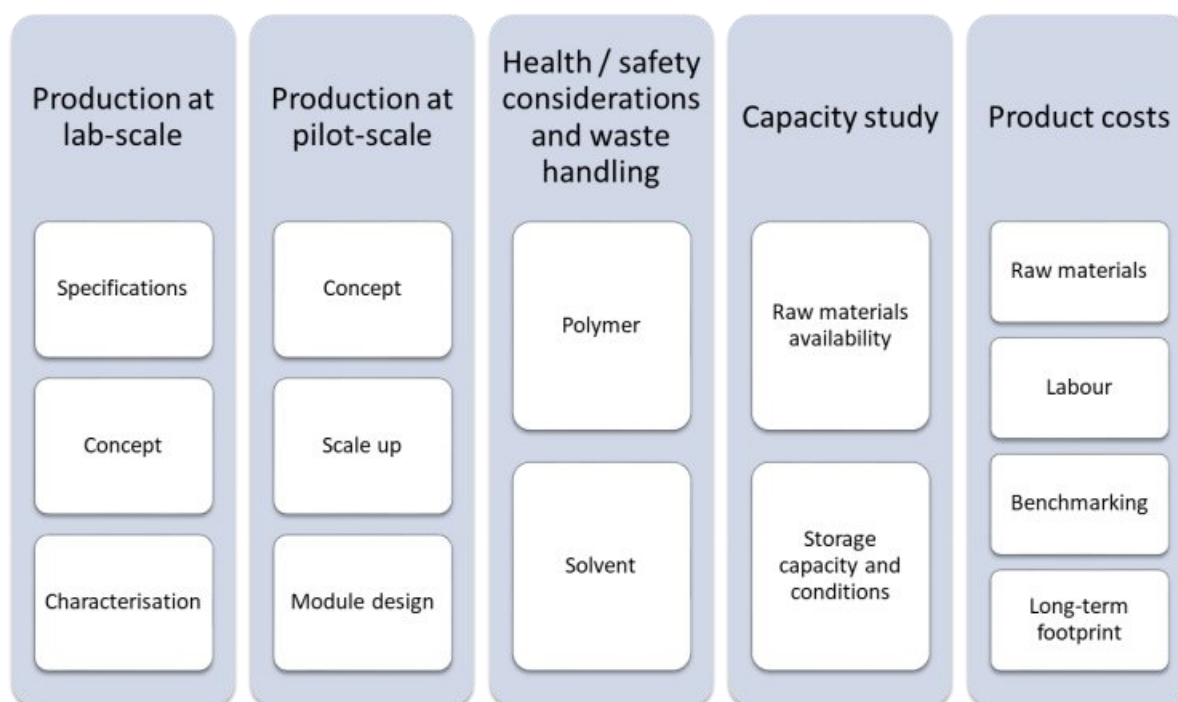
Figure 1 - An overview of the scalability analysis.

# 3  Ion exchange resins

The implementation of tailor-made ion exchange resins was previously planned for Case Study 3: Simultaneous metal recovery and wastewater treatment in plastic electroplating production. In this regard, the planned metal recovery plant was designed as a central unit that treats wastewater from all copper, nickel and chromium containing baths of the BIA production plant in Solingen. As depicted in Figure 2, the unit consists of a prefiltration section, an ion exchanger section and a reverse osmosis section. Wastewater will be discharged every 2-3 days and collected in tanks (one tank for each metal, three in total). It is first subjected to prefiltration and the resulting filtrate is directed to an activated carbon bed to remove organic compounds such as surfactants and other additives. The key of the proposed process is to use ion exchange resins to control both the neutralization and the pH value.

This in turn avoids the introduction of foreign ions due to external neutralization using sodium hydroxide. After organic compounds removal, metal sulfate ions are adsorbed in a cation exchanger (CEX, in $H^+$ form) and sulfate ions are adsorbed in anion exchanger in (AEX I, $OH^-$ form) leading to the equimolar release of protons and hydroxide ions (no pH change). The resulting effluent is treated at a batch reverse osmosis unit. Clean water (permeate) is collected in a tank and reinjected in the rinses. The resulting retentate mostly consists of concentrated boric acid, which is collected and reused to refresh the treatment bath.
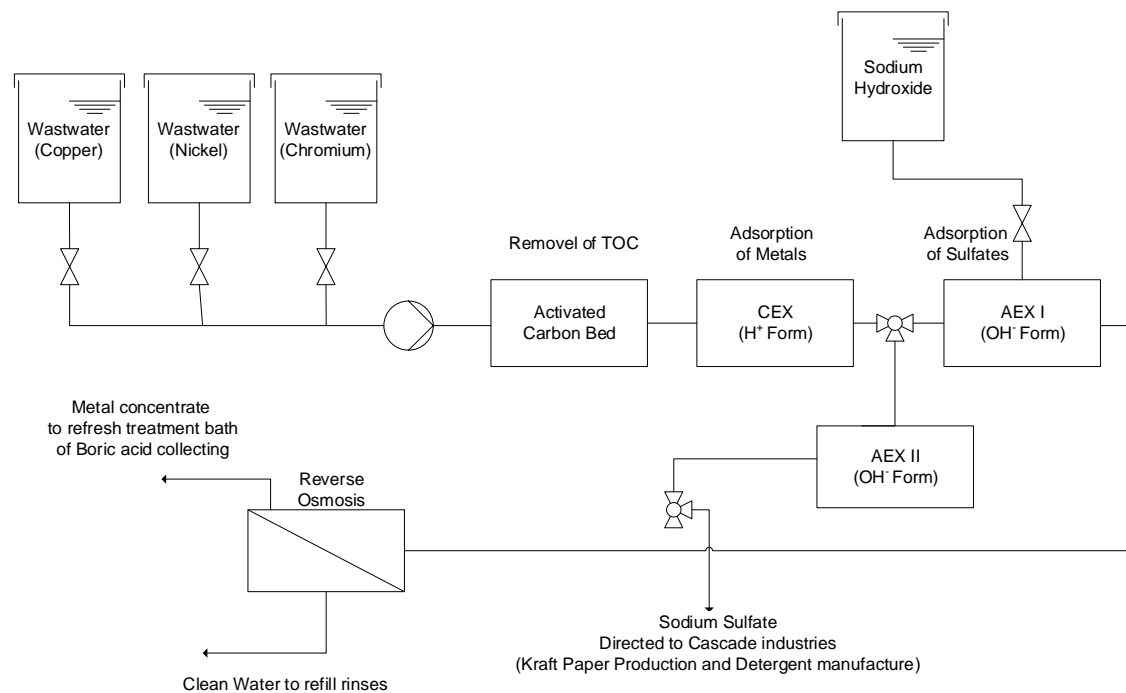
Figure 2 - Process diagram of the simultaneous metal recovery and wastewater treatment to be implemented in Case Study 3.

In CEX, metals are eluted by means of sulfuric acid. In this step, metal ions are exchanged by proton and it is crucial to eluate at low sulfuric acid concentration in order to avoid strong acidification and sulfate ions excess. The eluate is then directed to a second anion exchanger (AEX II, OH- form) where excess sulfate ions are absorbed leading to the release of hydroxide ions and the neutralization of the eluate from CEX. This stream is finally concentrated by means of batch reverse osmosis to reach the specified electrolyte concentration. AEX I and II are regenerated by means of a sodium hydroxide solution leading to the release of sodium sulfate ions which can be used in cascade processes such as Kraft paper or detergent production.

In the meantime, new progress was achieved in the field of sulfate ions recovery from process water by means of commercially available ion exchange resins. Öztürk and Ekmekçi (2020) successfully demonstrated the utilization of Amberlite IRA-400 (DuPont[TM]) and Dowex 1X2 (Dow Inc.) for the removal of sulfate ions from process water. In this study, Amberlite IRA-400 showed excellent adsorption kinetics and upscaling can be easily performed by adapting the required quantity of resin according to the concentration of dissolved ions in the process water. In this study, resin regeneration was achieved by means of 4% w/v NaOH solution and repeated adsorption/elution cycles were successfully ran. Commercially available chelating exchange resins, such as Diaion CR11 (Mitsubishi Chemical Corporation) or Amberlite IRC-718 (DuPont[TM]), as well as weak cationic resins such as Amberlite IRC86 (DuPont[TM]) are known to work well for the efficient adsorption of heavy metals (chromium, nickel and copper) from electroplating wastewater (Cavaco et al., 2007; Yalçin et al., 2001).

Based on the preliminary studies conducted at lab scale, the commercially available ion exchange resins are well suited for the requirements of intelWATT processes.

# 4  Membrane production concept

## 4.1  Specification requirements

An overview of the membrane specifications for the MD/MCr process currently used in literature and the recommended values is presented in Table 1 (Eykens et al., 2017). The ideal membranes for this purpose must be hydrophobic in order to achieve wetting resistance, and have appropriate porosity and pore diameter to accomplish flux efficiency, without being compressible.

Table 1 - Required specifications of MD and MCr membranes.

| Parameter | Affected parameters | Range used in literature | Recommendation |
|---|---|---|---|
| Contact angle (θ) | Wetting resistance | 80-160° | >90°<br>As high as possible |
| Liquid entry pressure (LEP) | Wetting resistance | 0.5-4.6 bar | >2.5 bar |
| Pore diameter | Wetting resistance Flux and energy efficiency | 0.012-1.2 μm | 0.1-1 μm |
| Porosity (e) | Flux energy efficiency, mechanical strength | 38-90% | As high as possible |
| Thickness (δ) | Flux, mechanical strength | 10-200 μm | As low as possible |
| Tortuosity (τ) | Flux energy efficiency | 1.1-3.9 | <2 |
| Thermal conductivity of the material ($\kappa_m$) | Flux energy efficiency | 0.031-0.057 W m$^{-1}$ K$^{-1}$ | As low as possible |
| Tensile strength | Mechanical strength | 3.4-57.9 MPa | >10 MPa |
| Compression | Flux and energy efficiency at full scale, mechanical strength | PTFE: 22% at 0.6 bar | Not compressible |

In this report, PVDF, a semi-crystalline thermoplastic fluopolymer is used as a membrane material owing to its capability of membrane formation, its good mechanical properties as well as its intrinsic excellent chemical resistance against corrosive chemicals, thermal and chemical stability and highly hydrophobic nature. In addition, the copolymer PVDF-HFP is tested as membrane because presents lower crystallinity and higher free volume compared to PVDF homopolymer, due to the incorporation of an amorphous phase of HFP into the main constituent VDF blocks. The fluorine content also increases due to the addition of HFP group, which makes PVDF–HFP more hydrophobic than PVDF, making it a potential candidate for some applications where increased hydrophobicity of the membrane material is required due to process restrictions, e.g., high pressure. Apart from the excellent material properties of PVDF and PVDF-HFP, NSCR has previous experience and know-how on the production of membranes with these polymers (Athanasekou et al., 2019).

The PVDF-based membranes are produced via phase inversion methods due to their simple processing, flexible production scales and low cost. In these methods, the PVDF solution (dope liquid) is cast onto a flat surface and then immersed in adequate nonsolvent bath ($H_2O$). A solvent/nonsolvent exchange takes place and, once passed a critical composition, the polymer solution becomes thermodynamically unstable and

faces a liquid-liquid phase separation. In the case of hollow fiber preparation, the nonsolvent used is the bore liquid and the external coagulant is tap water. The experimental phase equilibrium data at 25 °C for PVDF in water/NMP solutions are presented in Figure 3. The open circles represent the gelation compositions for PVDF in water/NMP solutions. For each system, the gelation points form a phase boundary, below which gelation will take place for a dope standing at 25 °C over an extended period of time.
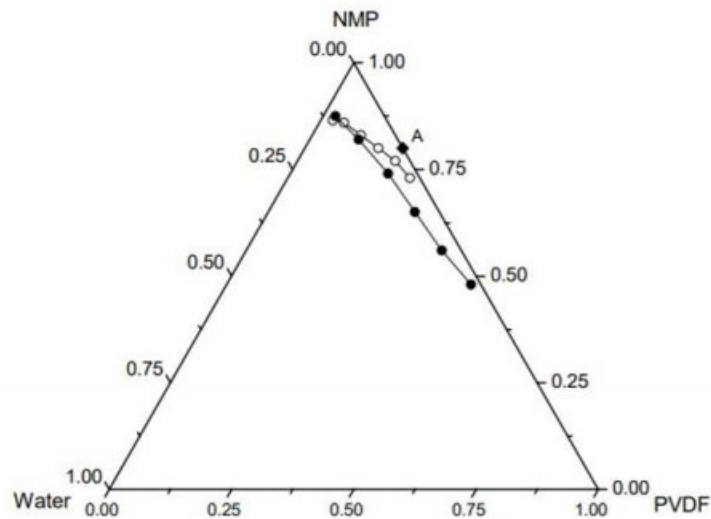


Figure 3 - Phase diagram of water-NMP-PVDF system, -○-: gelation line; -●-: binodal

The quality of the produced membranes is evaluated in terms of morphology (SEM), water contact angle (WCA), liquid entry pressure (LEP), overall porosity, pore size distribution and thickness. Upon successive increments the LEP was defined as the pressure at which a continuous liquid flow was maintained through the outlet port of the vessel. This critical pressure difference is related to the surface tension of the fluid $\gamma_L$ (N.m$^{-1}$), the maximum pore radius $r_{max}$ (m), the fluid contact angle θ (○) and assumes an intrinsic parameter for the pores' geometry B (-) (Rácz et al. 2014). The calculation of this parameter is based on Franken equation, which is equivalent to Young –Laplace equation. In this case, the parameter B=1, the equation has the form:

$$LEP = \frac{-2\gamma_L cos\theta}{r_{max}} \quad (1)$$

LEP values for membranes with WCA less than 90° and is explained on the basis of the Purcell model taking into account the toroid shape of the pores. Specifically, the Purcell model is described by the following two equations:

$$\Delta P = \frac{-2\gamma}{r_p} \cdot \frac{cos(\theta+\alpha)}{1+ R/r_p(1-cos(a))} \quad (2)$$

$$\sin(\theta + \alpha) = \frac{\sin(\theta)}{1+ r_p/R} \quad (3)$$

where $R$ is the fiber radius and $\alpha$ is the angle below horizontal at which the liquid meniscus pins prior to break-through.

The porosity ($\varepsilon$) can be determined by the gravimetric method, as defined in the following equation:

$$\varepsilon = \frac{((w_{e+p}-w_p)/\rho_e}{(w_{e+p}-w_p)/p_e+w_p/p_p} \quad (4)$$

Where, $w_p$ and $w_e$ are the mass of sample and isopropanol, while $p_p$ and $p_e$ are the density of the sample and isopropanol, respectively.

## 4.2 Hollow fiber membrane preparation at lab scale

Hollow fiber membranes are typically fabricated via the solvent-induced phase separation method (SIPS). To ensure that they have desirable pore size, narrow pore-size distribution, ultra-thin selective layer and open-cell sponge-like substructure morphology to maximize separation performance, a number of parameters must be optimised. Figure 4 illustrates a typical spinning line for the fabrication of polymeric hollow fibers and Figure 5 shows an enlargement of the region with the spinneret. Once the dope solution is prepared and degassed, the hollow fiber spinning process usually consists of the following steps: (1) feeding of the spinning dope and bore liquid through a spinneret; (2) spontaneous coagulation of the dope solution in contact with the bore fluid upon exiting the spinneret, preventing the collapse of the lumen side; (3) solvent evaporation from the outer nascent membrane surface in the air-gap region; (4) moisture-induced early phase separation in the outer nascent membrane surface in the air-gap region; (5) solidification-formation of the fiber and completion of phase inversion induced by the external coagulation bath (water); and (6) solvent exchange and additional post-treatment.


(A)


(B)
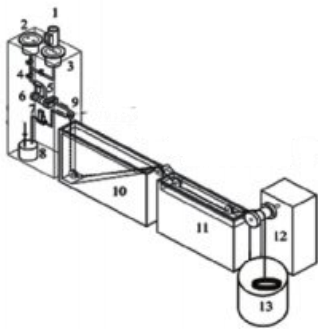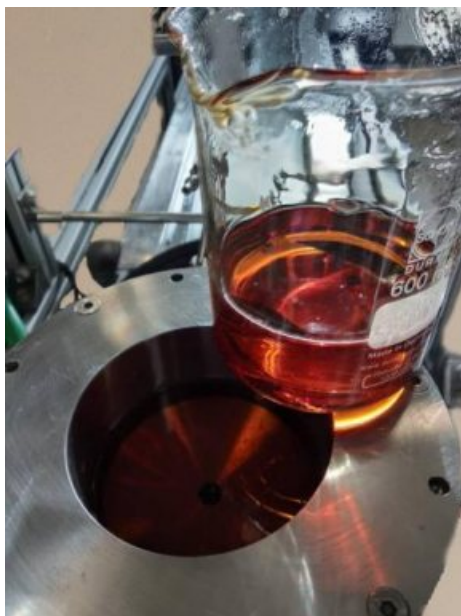
Figure 4 - Hollow fibers lab-scale preparation setup. (A) Schematic representation of spinning setup: 1 Mechanical stirrer, 2 Dope solution tank, 3 Mixing tank, 4 Valve ,5 Filter, 6 Gear pump, 7 Pump inverter, 8 Bore liquid tank, 9 Spinneret, 10 and 11 Coagulation baths, 12 Motor guide and 13 Storage tank. (B) Spinning apparatus. (C) Dope solution into tank. (D) Coagulation bath with motor guide.
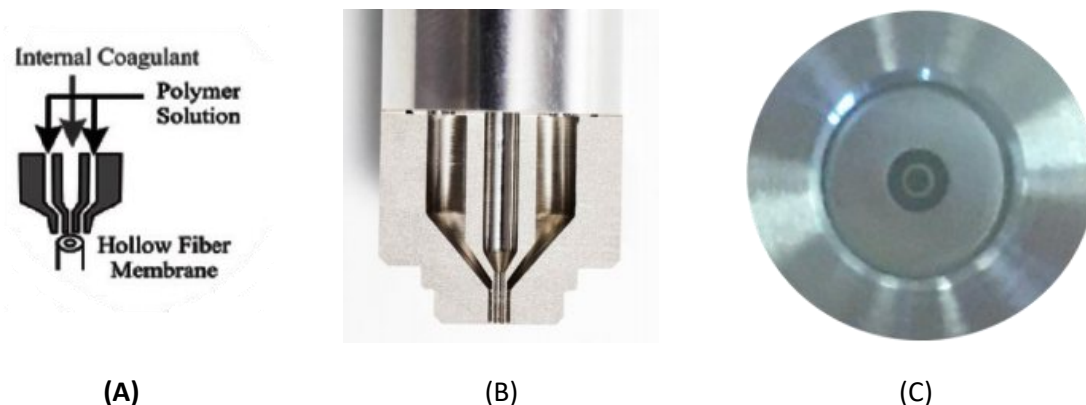


**(A)** **(B)** **(C)**

Figure 5 - (A) Schematic and (B) photographic longitudinal section of a spinneret nozzle. (C) Picture of the spinneret's double orifice.

PVDF hollow fibers are prepared by wet spinning (without air gap) phase inversion process using the tube-in-orifice spinneret of Figure 5. The internal and external diameter of the internal tube (needle) is 500 µm and 700 µm, respectively and the internal diameter of the external tube (orifice) is 1200 µm. In Table 2 the experimental parameters of preparation PVDF-based hollow fibers membranes are presented (Balis et al., 2019).

Table 2 - Experimental parameters of preparation of PVDF-based hollow fiber membranes.

| Parameters | PVDF | PVDF-HFP |
|---|---|---|
| Dope solution PVDF/NMP (PVDF-HFP/NMP) (wt.%) | 17/83 | 30/70 |
| Bore liquid NMP/$H_2O$ (wt.%) | 80/20 | 80/20 |
| Dope solution flow rate (mL/min) | 4.2 | 4.2 |
| Bore liquid flow rate (mL/min) | 1.8 | 2.2 |
| Air gap (cm) | 0 | 0 |
| Dope solution temperature (°C) | 50 | 50 |
| Coagulation bath temperature (°C) | 25 | 25 |

## 4.3  Flat sheet membranes preparation at lab scale

The procedure for the PVDF flat sheet membrane preparation is manual and encompasses the following steps: 15 g of the polymeric powder are dissolved into 80 mL NMP and the solution is mixed at 50 °C. The solution is stirred for at least one day to guarantee complete dissolution of the polymer and subsequently is stabilized by bath sonication for 3 h at 50 °C. The dope solution is cast uniformly onto a glass substrate by means of a hand-casting knife adjusting the wet thickness to 100 µm and then is immersed in a coagulation

bath after exposure for a fixed time to the air. After complete coagulation, the membranes are transferred into a pure water bath, where they are kept till use. The membranes are stored in a deionised water bath until tested, having an average thickness of 50 µm.

For the preparation of porous PVDF-HFP membranes the procedure described below is followed: PVDF-HFP is dissolved in acetone at 40 °C to prepare a 5% wt.% stock solution. Deionized water (2 wt. %) is added under agitation, until the solution becomes homogeneous. After 1 h, the solution is cast onto a clean glass plate, or a PP non-woven fabric, e.g. Novatex 2473, using a hand-casting knife with a 100 µm gap. After the evaporation of acetone and water is completed, opaque membranes are obtained. Table 3 shows the parameters of the produced membranes.

Table 3 - Typical parameters of PVDF-based flat sheet membranes.

| Parameters | PVDF | PVDF-HFP |
|---|---|---|
| Polymer solution PVDF/NMP/$H_2O$ (PVDF-HFP/acetone/$H_2O$) (wt.%) | 15/85/0 | 5/93/2 |
| Polymer solution temperature (°C) | 50 | 40 |
| Coagulation bath | $H_2O$ | - |
| Coagulation bath temperature (°C) | 25 | - |

## 4.4  Characterisation of membranes

The SEM micrographs presented in Figure 6 show the morphological characteristics of PVDF hollow fibers. Figure 6 (A, B) shows that the prepared hollow fibers have outer diameter (OD) ~1000 µm, wall thickness ~200-250 µm and inner diameter (ID) ~500-550 µm. PVDF hollow fibers constitute of narrow sponge-like regions between the fingers (Figure 6B). Also, the pores of the membranes present small size and thickness in the sponge-like structure (Figure 6C). Figure 7 shows the morphological structure of PVDF flat sheet membranes with a spongy and porous cross-section surface similar to the membranes found in literature.
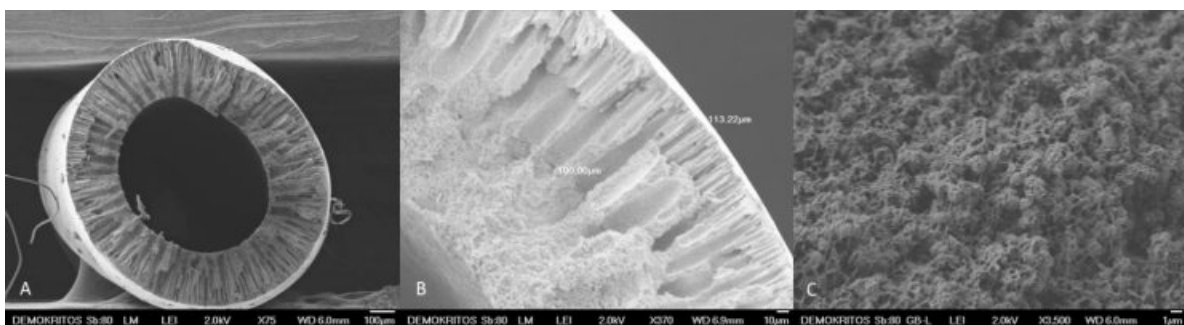


Figure 6 - SEM micrographs of the PVDF hollow fibers. (A) Full cross section (magnification 75x), (B) part cross section (magnification 370x) and (C) enlarged cross section (magnification 3500x).
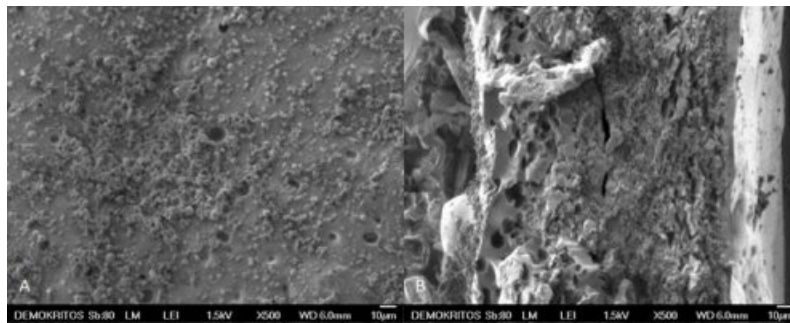
Figure 7 - SEM micrographs of the PVDF flat sheet membranes: (A) Top surface and (B) Cross-section.

The typical properties of the hollow fibers are shown in Table 4 and of flat sheets in Table 5.

Table 4 - Typical properties of the lab-scale hollow fiber membranes.

| Sample | LEP (bar) | CA (°) | Porosity (%) | Wall thickness (µm) | Pore size (µm) |
|---|---|---|---|---|---|
| PVDF | 2.5 ± 0.5 | 95 ± 5 | 70 ± 5 | 225 ± 25 | 0.4 ± 1.5 |
| PVDF-HFP | 4 ± 0.5 | 95 ± 5 | 55 ± 5 | 225 ± 25 | 0.2 ± 1.5 |

Table 5 - Typical properties of the lab-scale flat sheet membranes.

| Sample | LEP (bar) | CA (°) | Porosity (%) | Thickness (µm) | Pore size (µm) |
|---|---|---|---|---|---|
| PVDF | 2.7 ± 0.5 | 92 ± 3 | 65 ± 5 | 150± 5 | 0.5 ± 0.7 |
| PVDF-HFP | 2.5 ± 0.5 | 120 ± 5 | 60 ± 5 | 50 ± 5 | 0.2 ± 1.5 |

# 5  Membrane production scale-up

## 5.1  Hollow fiber membrane production process at pilot scale

The production of hollow fiber membranes at pilot scale will take place with the same apparatus used at lab scale, with several necessary modifications. The purpose of the modifications is to face the main two constraints of the current lab-scale apparatus:  limited speed of production and dependence on manual labour.

The first challenge to address is the limited volume of the dope solution tank. Its current lab-scale capacity is 400 mL, allowing for a single batch production of 200 m (or 0.6 m$^2$ cell-side area) of hollow fibers. The duration of each batch, including 90 min for preparation and cleaning, is 180 min, allowing for 2 batches per day.

A larger dope solution tank is necessary for the pilot scale to function in a single batch per day and reduce the need for labour-intensive cleaning of the apparatus required between each batch, assuming 1 mm outer diameter. A full-day 6-h duration batch (including preparation and cleaning) would require a dope solution volume of 1,100 mL and would increase the batch size to 550 m (or 1.7 m$^2$ cell-side area). Although this simple modification would permit to keep the current bore liquid tank of 600 mL, the same spinneret and the existing pumps, the speed of production is limited by the flow rate of the solutions.

A more productive option would require a larger flow rate of the dope solution and the bore liquid. In order to achieve this without increasing pressure, apart from adjusting/replacing the pumps, it would be necessary to have a larger orifice spinneret. By doubling the outer diameter to 2 mm, production of the double membrane area per unit of length would be allowed, however this would also double the polymer and the solvent needed, 22 kg and 108 kg in total, respectively, if the membrane thickness doubled too. A dope solution volume of 2,200-2,700 mL would be consumed in a 6-h batch (including preparation and cleaning), but the length produced per batch would be only 275-340 m. This option would further require the replacement of the bore liquid tank. It must be noted that an adjustment of the motor speed in combination with the larger spinneret, could increase production, provided that the membrane characteristics would remain unchanged, which needs to be verified. Otherwise, the previous option is more preferable. The above-mentioned options are summarised in Table 6. The amounts of polymer and solvent that are wasted during production are not included in the table and account for around 20% based on lab-scale calculations.

Table 6 -Parameters of hollow fiber membranes' production at lab and pilot scale.

| Parameters | Lab Scale (OD = 1 mm) | Pilot Scale (OD = 1 mm) | Pilot Scale (OD = 2 mm) |
|---|---|---|---|
| Total membrane area | 100 m$^2$ | 100 m$^2$ | 100 m$^2$ |
| Membrane length | 0.5 m | 1 m | 1 m |
| Cell-side area of each fiber | 0.0016 m$^2$ | 0.0031 m$^2$ | 0.0062 m$^2$ |
| Total number of fibers | 62,500 | 32,000 | 16,000 |
| Total length of fibers | 32,000 m | 32,000 m | 16,000 m |
| Number of 150-fiber modules | 417 | 213 | 107 |
| Dope solution flow rate | 4.2 mL/min | 4.2 mL/min | 8.4-10.0 mL/min |
| Bore liquid flow rate | 1.8 mL/min | 1.8 mL/min | 3.6-5.0 mL/min |
| Volume of dope solution per batch | 400 mL | 1,100 mL | 2,200-2,700 mL |
| Length of fiber per batch | 200 m | 550 m | 275-340 m |
| Duration of 1 batch (+preparation/cleaning time) | 180 min | 360 min | 360 min |
| Number of batches per 6-h day | 2 | 1 | 1 |
| Membrane area produced per day | 1.2 m$^2$ | 1.7 m$^2$ | 1.7-2.1 m$^2$ |
| Total PVDF consumption | 11 kg | 11 kg | 22 kg |
| Total NMP consumption | 55 kg | 54 kg | 108 kg |

The second modification is related to the winding of the fabricated hollow fibers at the end of the process, which is currently performed manually. The manual option, apart from being very laborious, involves a higher risk of damaging the fibers and does not guarantee the uniformity of the fiber thickness, since the speed of winding can affect the thickness. A spool is necessary for automated winding of the fibers while keeping them underwater, with as less as possible human intervention. Some examples of spools can be seen in  Figure 8Figure 8.

Figure 8 - Examples of spools for winding hollow fibers.

Ideally the spool should be large enough to accommodate for the full length of the fibers of every batch. The surface of the spool can have ridges in the form of a helix, similar to screw threads, to drive the fibers in a uniform manner at a single layer and eliminate any damage of the fibers' surface. In order to fit the full length of one batch (300 m) of fibers at one layer on the spool (50 cm diameter) its width should be around 50 cm. The spool should be partly emerged in water, so a large storage tank is also necessary. The spool will be connected to the motor guide through a roller chain to secure the same linear velocity for the fibers. A schematic representation of the winding system is presented in Figure 9.
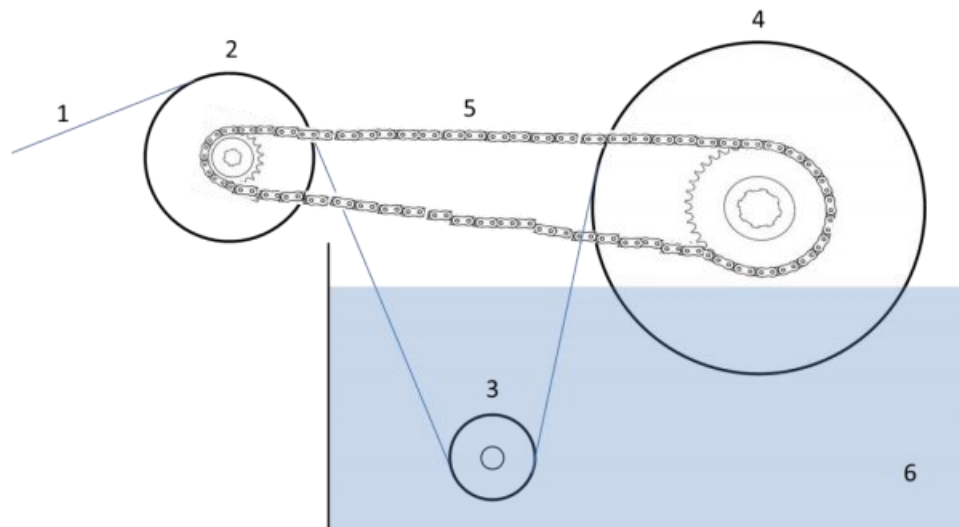


Figure 9 - Schematic representation of the system for automated winding of hollow fibers: 1 the fabricated hollow fibers coming from the washing bath, 2 motor guide, 3 guide, 4 spool, 5 roller chain, 6 storage tank.

## 5.2 Flat sheet membrane production process at pilot scale

For a semi-continuous production of flat sheet membranes, the lab-scale casting system cannot be adapted, therefore a casting machine with a roller is necessary. The concept of this apparatus is that a thin film (50–100 μm) of polymer solution is applied on top of a smooth, non-woven and very permeable fabric made from polymer fibers – it is strong but offers hardly any resistance to mass transfer. The thickness is adjusted by a blade, i.e., the casting knife. Once the polymer film enters a coagulation bath (typically water) the organic solvent of the polymer dissolves in the bath whilst the polymer itself does not, i.e., precipitation occurs. The process depends on operating parameters such as velocity of the casting process, composition

and viscosity of the solution or temperature of the coagulation bath. The result is an asymmetric flat sheet membrane. Figure 10 shows the schematic drawing of a membrane casting machine (Abetz et al., 2021).
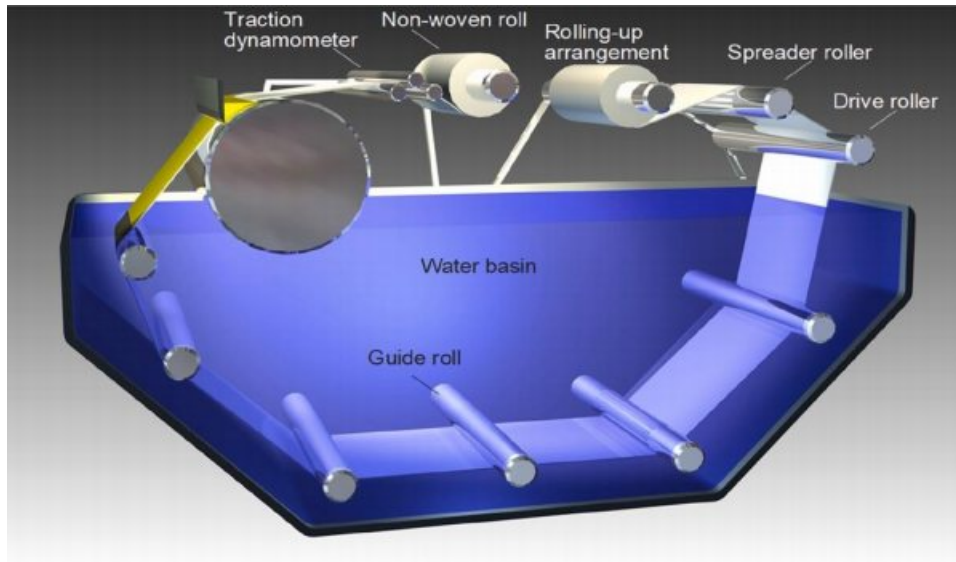


Figure 10 - Schematic representation of a membrane casting machine for the production of flat sheet membranes (Abetz et al., 2021).

The specifications of a semi continuous casting system from PHILOS Co., Ltd., Republic of Korea, are presented below as an example. The standard maximum casting width provided is 35 cm but it can be customised for the requirement of 40 cm.

System dimension

- Casting system: 1,730 mm L x 500 mm W x 760 mm H

Unwinding unit
- Un-winder diameter: Max. 200 mm D
- Roll core chucking: manual operation

Casting unit

- Casting device: blade type doctor knife and thickness control by μm with thickness gauge
- Range of the casting thickness: 0-10mm
- Minimum casting layer thickness: 50$\mu m$
- Accuracy of the coating layer thickness: ±5$\mu m$
- Casting solution range: 2,500-10,000 cps
- Fabric width: maximum 350 mm
- Material: stainless steel 304

Coagulation and washing unit
- Bath dimension: 1,000 mm L x 400 mm W x 330 mm H
- Material: tank (stainless steel 304), frame (aluminum profile)
- Temperature control range: room temperature (option: heat exchanger connection possible)

Guide roller
- Material: stainless steel 304
- Dimension: 42 mm D x 370 mm L

Rewinding unit
- Winder speed: adjustable in the range of 0.2-1 m/min, changeable by customer's requirement
- Rewinding diameter: max. 200 mm D
- Roll core chucking: manual operation

System power and control
- AC 220 V x 50/60 Hz, 1.5 kW

The total price, including online (due to COVID-19 restrictions) operation support, training, and technical service, exclusive of tax/VAT and shipment is 49,500 USD (approx. 42,000 EUR) for 35 cm width and 57,000 USD (approx. 48,400 EUR) for 40 cm width. The time of manufacturing is 90-120 days.



Figure 11 - PHILOS semi continuous flat sheet membrane casting system (only for reference).

The membrane production parameters in lab scale (batch) and pilot scale (semi continuous) are presented in Table 7. In both scales, the dimensions mentioned and the amounts of polymer and solvent consumed for their production refer to the effective area of the membranes. Thus, while the pilot-scale sheets have an effective area of 65 x 35 cm, their overall surface area is 70 x 40 cm, which increases the raw material needed by 22%. The production speed at pilot scale is based on the winder speed and includes a preparation and cleaning time of 1.5 h per 6-h day.

Table 7 - Parameters of flat sheet membranes' production at lab and pilot scale.

| Parameters | Lab Scale (30 x 20 cm) | Pilot Scale (65 x 35 cm) |
|---|---|---|
| Total membrane area | 100 m$^2$ | 100 m$^2$ |
| Area of each sheet | 0.06 m$^2$ | 0.23 m$^2$ |
| Total number of sheets | 1667 | 435 |
| Total length of non-woven roll | 500 m (20 cm wide) | 286 m (35 cm wide) |

| | | |
|---|---|---|
| Production speed per day | 0.12 m$^2$ | 21-108 m$^2$ |
| Total PVDF consumption | 7.5 kg | 7.5 kg |
| Total NMP consumption | 42.5 kg | N/A |

## 5.3 Module design, construction and use

### 5.3.1 Hollow fiber modules

In WP 4 the project partner NCSR develops membranes for MD. In order to be able to conduct a preliminary membrane screening (WP 3), the hollow fiber membranes were inserted into modules by project partner CUT. For this screening, the modules were designed and built for a DCMD (Direct Contact Membrane Distillation) process.

Research and Development was done regarding mechanical stability of module components (glue, housing material, etc.) and the processability of the membranes in the production process.

The module design is a decisive criterion for the efficiency of the subsequent membrane processes. An important aspect which should be considered when developing modules concerns the stability of the module components under the prevailing process conditions. Especially the temperatures of up to 80 °C envisaged in the process must be considered for the selection of module components. So are often used housing materials, such as PVC-U only applicable up to a temperature of 60 °C. The same applies to the potting material, the bonds and the seals.

Regarding the housing, PVC-C was selected, which due to its high chlorine content has increased chemical and thermal resistance in comparison to conventional PVC-U. After some necessary treatment also a very strong adhesion of the resin to the housing material can be achieved.

The standard CUT laboratory or test module was chosen as the basis for the DCMD module (see Figure 12) and adapted in terms of construction and material selection.
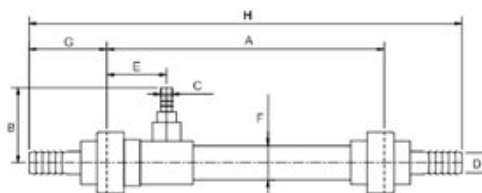


Figure 12 - General drawing of CUT standard lab- (art.no. 760265) and test-module (art.no. 760266).

The most important corresponding dimensions are shown in Table 8.

Table 8 - Important dimensions of the lab- and test-modules presented in Figure 12.

| | | Art.no. 760265 | Art.no. 760266 |
|---|---|---|---|
| Length (mm) | [A] | 500 | 1.000 |
| Total length (mm) | [H] | Approx. 678 | Approx. 1.190 |
| Module Diameter (mm) | [F] | 40 | 50 |

In the DCMD process, two process streams, the warm, salty water (lumen of the membrane) and the cold water (shell side), pass each other in countercurrent. To do this, a second permeate outlet had to be added

to the standard module. The second permeate outlet was installed in a so-called Z-configuration in order to guarantee an even cross-flow and temperature distribution in the module (see Figure 13).



Figure 13 - CUT lab test module (art.no. 760265) with two permeate outlets in Z-configuration.

Membrane modules were built with two generations of MD membranes, which CUT received from NCSR. The manufacturing process comprises following steps:

1. Sealing of the membrane ends in order to prevent resin from penetrating into the open membrane ends during potting.

2. Insertion of the bundle into the module.

3. Attachment of the casting molds and insertion of the resin in static potting process.

4. After curing the module is demolded, excess resin is removed and thus the membrane ends are opened (Figure 14Figure 14).
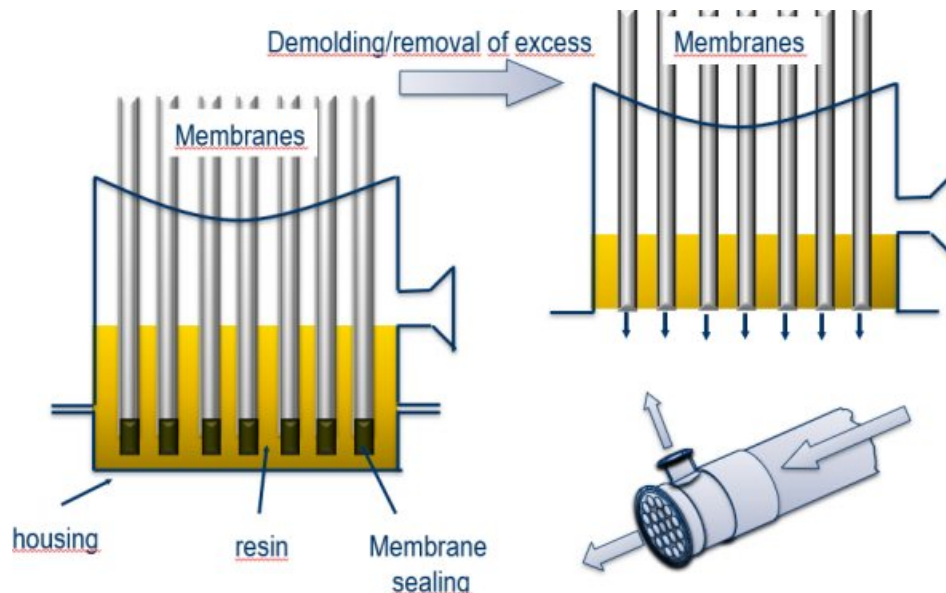


Figure 14 - Scheme of capillary module production.

The first generation of membranes (Figure 15) proved unfortunately difficult to handle, since the membranes were soft and easy to kink.

958454 — intelWATT        D4.4 -     Report on scalability of ion exchange and MD/MCr membranes        22/35
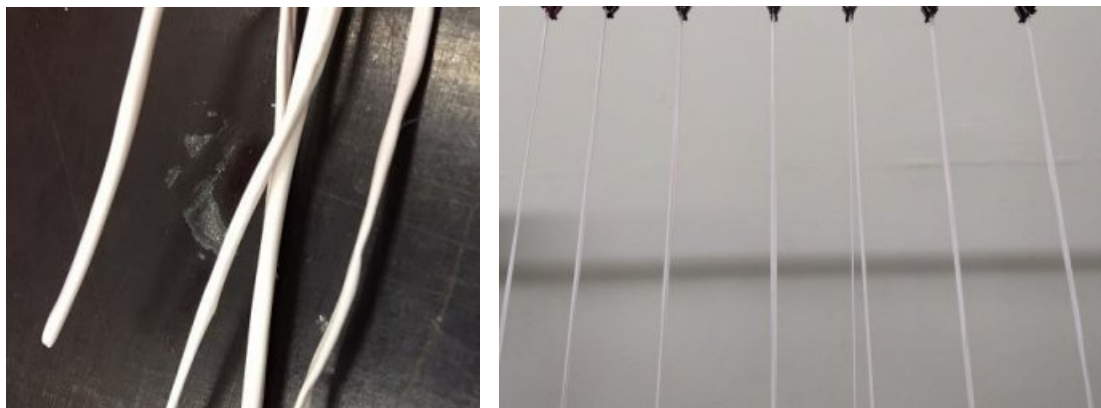
Figure 15 - Hollow fiber membranes from the first generation (left) and from the second generation (right).

For that reason, the delivered membranes had to be sort out before module production. During the production the membranes had to be handled very carefully. The finished module (Figure 13) contained 150 active membranes, which results in a membrane area of 0.22 m$^2$. The module was sent to NCSR and CNR-ITM for further testing of its performance.

The second-generation membranes proved to be more stable than the first. A few membranes still had to be sorted out, but handling was much easier. Two different modules were built. The longer of the two was sent to the project partner NCSR for further evaluation (Figure 16). The shorter module was made available to the project partner CIEMAT to evaluate the thermal and separation efficiency in their MD plan.



(A)                                                                                              (B)
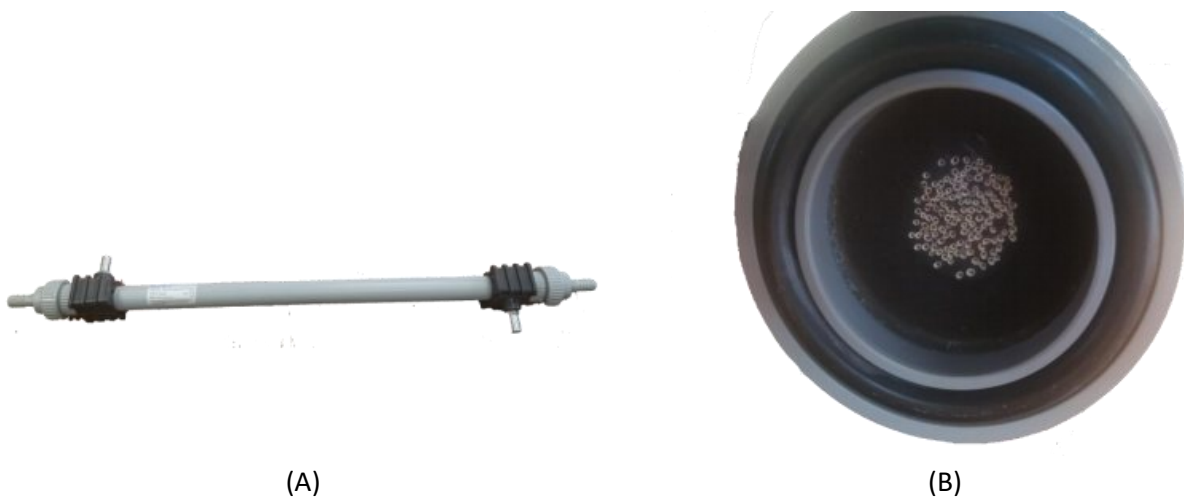
Figure 16 - CUT pilot test module (art.no. 760266) with two permeate outlets in Z-configuration.

Table 9 gives an overview of the built modules.

Table 9 - Overview of the built modules and corresponding membrane areas.

| Module art. No. | Membrane generation | Number of membranes | Membrane area [m$^2$] |
|---|---|---|---|
| 760265 | 1$^{st}$ | 150 | 0,22 |
| 760265 | 2$^{nd}$ | 150 | 0,20 |
| 760266 | 2$^{nd}$ | 133 | 0,37 |

## 5.3.2 Flat sheet modules

The evaluation of flat sheet membranes performance at lab scale is tested by using modules as shown in the Figure 17 with dimensions A) 21 x 30 cm and B) 5 x 5 cm.
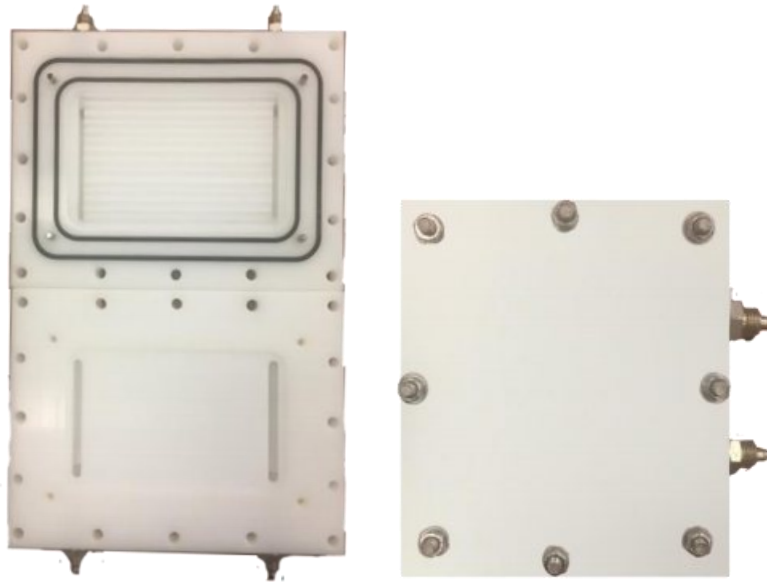


Figure 17 - Lab-scale flat sheet membrane modules, 21x30 cm (left) and 5x5 (right).

The goal of the project is to scale up the dimensions of the membrane to effective area of 35 x 65 cm by using modules with multiple stages, such as Memsys frames shown in Figure 18. (Zhao et al., 2013).



(A)                                    (B)                                    (C)
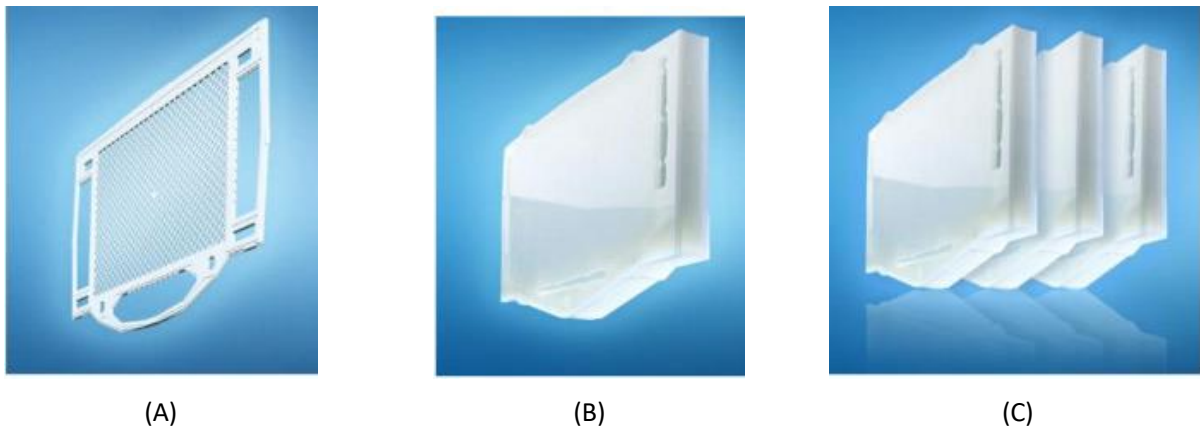
Figure 18 - Photos of Memsys frame and stages. (a) Frame, 2 pieces of membranes or PVDF were weld onto both sides of the frame; (b) single stage with welded frames and two covering plates; (c) multiple stages.

# 6 Health and safety considerations and waste handling

## 6.1 Considerations for PVDF

Incineration of PVDF generates hydrogen fluoride (HF) gas, the inhalation of which can cause moderate to severe health effects. Although incineration of PVDF is not expected to take place neither during the production process nor as a method of waste management, in case PVDF is to be incinerated, it must take place in appropriate facilities in which HF gas can be neutralized. All the people involved in the production and use of PVDF membranes must be informed about the potential risks in case of a fire accident.

### 6.1.1 Polymer recycling

Based on lab-scale fabrication of membranes, we calculated that approximately 20% of PVDF used for the fabrication of membranes is wasted during preparation and cut-off of flat sheets and hollow fibers, during module preparation and with the rejection of defected membranes.

PVDF can be collected and either sold to companies who buy scrap or regrind PVDF, or internally recycled for the production of membranes in combination with new PVDF. Alternatively, it can be collected as waste with a price of approximately 0.8 EUR/kg, but this option is the least favourable.

The price for selling PVDF scrap depends on the size of the scraps, on the purity of the polymer, on its colour and on the total quantity. However, the transport costs may render this option less advantageous.

It is possible to fabricate membranes from recycled PVDF. Wang et al. (2017) prepared hollow fiber membranes from recycled PVDF and achieved membranes with higher porosity, better permeability and similar wettability compared to normal PVDF membranes. However, the mechanical properties and BSA rejection were lower.

A pending patent (Ren et al., 2014) describes a recycling method of waste PVDF flat sheet membranes and of the non-woven supporting layer. The method comprises the following steps: firstly, removing contaminants from the surface of the waste membrane; drying the waste membrane and then dissolving the waste membrane in an organic solvent; performing solid-liquid separation on the PVDF so as to obtain a PVDF extracting solution and a non-woven fabric; filtering and removing impurities from the PVDF extracting solution by high-speed centrifugation or by using a filter membrane; adding partially fresh PVDF resins, pore-foaming agents, additives and the like into the PVDF extracting solution so as to prepare a membrane casting solution; preparing a regenerated flat sheet membrane by using a nonsolvent induce phase separation (NIPS) method; washing, drying and smashing the non-woven polyethylene terephthalate (PET); and then processing the non-woven PET into PET granules by using an extrusion melting method.

## 6.2 Considerations for NMP

NMP is hygroscopic but stable under normal conditions. It violently reacts with strong oxidizers such as hydrogen peroxide, nitric acid, sulfuric acid, etc. The primary decomposition products produce carbon monoxide and nitrogen oxide fumes. Excessive exposure or spillage should be avoided as a matter of good practice. NMP should be stored in clean, phenolic-lined mild steel or alloy drums. Teflon and Kalrez have been shown to be suitable gasket materials.

US EPA (2019) has issued a detailed risk evaluation for NMP. The agency assessed the impact of NMP on aquatic, sediment-dwelling species through surface water and sediment exposures, and to terrestrial species. After reviewing these data, EPA found no unreasonable risk to the environment. EPA found no unreasonable risks to the general population from any conditions of use. The general population could be exposed to NMP either through releases to water and air or through waste disposal. EPA found that it was unlikely the general population would be exposed to NMP through surface water, land-applied biosolids

and sediment. However, EPA found unreasonable risks to workers from 25 conditions of use of NMP. This chemical is commonly used commercially in the manufacture and production of electronics, agrichemicals, and petroleum products. Risks to workers can come from short-term and long-term inhalation, direct dermal exposure (through the skin) and vapor-through-skin exposure.

### 6.2.1  Protection measures

Good ventilation is necessary. "Local exhaust ventilation" is most effective. It captures NMP vapours at the source before workers breathe them. General ventilation using a fan-powered or heating, ventilation, and air conditioning (HVAC) system is the next best way to bring fresh air into the work area. Relying only on open doors and windows usually does not provide enough fresh air. Indoor fans that blow NMP-contaminated air around without removing it from the work area are not effective.

Respirators can be used to control harmful exposures only if ventilation and other control methods are not effective or feasible. A half-face respirator with organic vapor cartridges can reduce exposure. In spraying operations, this should be combined with a mist pre-filter. A dust mask does not remove NMP vapours from the air and does not protect workers. Respirators must fit properly and workers must be medically fit to wear a respirator.

Chemical protective utility gloves such as butyl rubber must be worn when using products that contain NMP. Gloves must be replaced often. Chemical protective clothing such as aprons, sleeves, boots, and head and face protection if NMP can contact skin at areas other than hands must also be used. The equipment must be cleaned thoroughly after each use.

### 6.2.2  Solvent recovery

NMP can be recovered from diluted aqueous solutions by distillation, taking advantage of the relative volatility difference between NMP and water. A patent by Miyata et al. (2012) describes a distillation apparatus for purifying spent NMP in a simple and safe manner irrespective of variation in concentration of water in a raw material or throughput, suitable for conducting automatic operation on-site. This distillation apparatus for NMP comprises a first distillation column in which the spent NMP is subjected to distillation and separated into a high-concentration NMP and water comprising low-boiling components; and a second distillation column in which bottoms from the first distillation column are further subjected to distillation and separated into a high-purity NMP and the high-concentration NMP comprising high-boiling components. However, distillation can be energy intensive, which can negatively affect operating costs and environmental impact.

Several low-energy separation methods have been discussed by Tozzi et al. (2018), such as solvent extraction, dividing wall columns (DWCs), heat pump assisted distillation (HPAD), vacuum distillation, pervaporation and cryogenic separation. Solvent extraction can be implemented more easily than the other alternatives that exhibit various limitations. Among several extracting solvents, chloroform shows high NMP recovery and is easy to separate and recycle from the extract stream using distillation. DWCs have been shown to reduce both energy expenditure and capital cost of the process equipment; however, appropriately designing a DWC for NMP recovery is very challenging. The HPAD and vacuum distillation reduce energy usage, but their solvent extraction performance is relatively low. Pervaporative recovery systems are costly.  There is lack of available data for NMP purification by cryogenic separation.

There are also several chemical filtration systems available that employ activated carbon, impregnated activated carbon, or ion exchange resins for the removal of NMP. Dallas et al. (2006) have evaluated several adsorbent materials, which are typically used in chemical filters to remove molecular bases and organics, for their ability to remove and retain NMP. Nonimpregnated activated carbon (NIC) with an optimized pore structure and surface chemistry has significantly more capacity for NMP than either citric acid impregnated activated carbon (LSP), or strong acid cation exchange resins (SACX). Even in accelerated tests, all three of

these adsorbents have excellent initial efficiency for NMP removal. The order of decreasing life for weak organic bases is expected to be NIC >> LSP > SACX. It was concluded that NMP interacts with all of the adsorbents through an equilibrium physisorptive mechanism that involves weak dispersive, dipolar, and hydrogen bonding interactions. It was also concluded that the adsorption of NMP on all of these adsorbents is not permanent. However, at the concentrations tested, the LSP adsorbs and retains weak organic bases the strongest at ambient conditions. These results suggest that the best chemical filter for weak organic amines would be a combination of NIC (capacity) and LSP carbon (retention).

Alternatively, NMP can be collected as waste with a price of approximately 0.8 EUR/kg, but this option is the least favourable.

### 6.2.3 Substitution of NMP

Most polymeric membranes are made from polymers that need to be dissolved in solvents such as NMP, *N*,*N*-dimethylformamide (DMF) and tetrahydrofuran (THF). These solvents are considered harmful in GSK's Solvent Selection Guide for Medicinal Chemistry and industry has been trying to avoid them in order to implement safer processes. Safer solvents like methyl and ethyl lactate, triethyl phosphate (TEP), dimethyl sulfoxide (DMSO), γ-butyrolactone (GBL), and ionic liquids (ILs) have been proposed for replacing the "classic" solvents in the phase inversion technique (Burgal et al., 2016). Some traditional, well-studied solvents for PVDF have green characteristics, while lesser-known green compounds are emerging as sustainable alternatives. While the definition of a green solvent is complicated, the most important sustainability metrics for PVDF processing are low-hazard and renewably sourced (bio-based). All solvents are bio-degradable, except the highly halogenated ones, with the exception of 1,4-dioxane, which is classed as a persistent bio-accumulative toxic (PBT) due to its stability in water (Marshall et al., 2021). Known solvents and green solvents are presented in Table 10.

Table 10 - Known solvents and green solvents for PVDF (Marshall et al., 2021).

| Solvent | Green solvent |
|---|---|
| Acetone | ✅ |
| Acetyl triethyl citrate (ATEC) | |
| γ−Butyrolactone (GBL) | ✅ |
| Cyclohexanone (CHO) | |
| Cyclopentanone (CPO) | ✅ |
| Dibutyl phthalate (DBP) | |
| Dibutyl sebacate (DBS) | |
| Diethyl carbonate (DEC) | ✅ |
| Diethyl phthalate (DEP) | |
| Dihydrolevoglucosenone (Cyrene) | ✅ |
| Dimethylacetamide (DMAc) | |
| N,N−dimethylformamide (DMF) | |
| Dimethylsulfoxide (DMSO) | ✅ |
| 1,4−Dioxane | |
| 3−Heptanone | |

| | |
|---|---|
| Hexamethyl phosphoramide (HMPA) | |
| 3−Hexanone | |
| Methyl ethyl ketone (MEK) | |
| N−methyl−2−pyrrolidinone (NMP) | |
| 3−Octanone | |
| Rhodiasolv® PolarClean | ✅ |
| 3−Pentanone | |
| Propylene carbonate (PC) | ✅ |
| Tetrahydrofuran (THF) | |
| Tetramethylurea (TMU) | |
| Triacetin | ✅ |
| Triethyl citrate (TEC) | |
| Triethyl phosphate (TEP) | ✅ |
| Trimethyl phosphate (TMP) | |
| N,N' tetrabutylsuccindiamide (TBSA) | ✅ |

Although literature provides some examples of PVDF membranes fabricated with different green solvents, further research is needed for a case-specific application, because the selection of solvent can have an impact on the properties of the membranes, including their performance.

# 7  Capacity study

## 7.1  Raw materials availability

Critical raw materials are raw materials with economic importance that have a high supply risk. Every three years the EU publishes a list of critical raw materials. PVDF, the main raw material used for the production of membranes, is synthesised by the polymerization of vinylidene fluoride (CH=CF). Fluorine is not in the list of 2020 critical raw materials (EU, 2020), therefore there is no critical raw material involved in the membrane production process.

The global PVDF market size is expected to increase from 0.9 bilion USD in 2020 to 1.4 billion USD in 2028, at a steady compound annual growth rate of 6.6%, according to Emergen Research (2021). High demand for PVDF from various end-use industries such as electrical, chemical processing, and construction is driving market growth to a significant extent over the forecast period. Robust performance and increasing adoption of PVDF in a range of applications such as membranes for water treatment is expected to continue to fuel growth of the PVDF market.

## 7.2  Storage capacity and conditions

The logistics for handling large volumes of membranes depend on the storage capacity. Apart from the limitations in storage space, is important to preserve the membranes in the same condition as they are in

the time of their production. The main problems related to the storage of PVDF membranes are photodegradation and drying.

According to photodegradation stability studies (Ong et al., 2017) cracks and fractures were detected on PVDF-based membrane surfaces when the membranes were exposed directly to UV light for up to 60 h. Furthermore, the mechanical strength and thermal stability of irradiated PVDF-based membranes was reported to decrease with increasing UV exposure time. Filtration experiments showed that the permeate flux of UV-irradiated PVDF membrane was significantly increased from approximately 11 to 16 L/m2.h with increasing UV exposure time from 0 to 60 h. Therefore, it is important to store the membranes in a dark environment and/or packaging material.

In order to prevent drying, the pores of PVDF can be filled with a solution of glycerin and non-solvent (water), which ensures an appropriate moisture content.  Prior to the use of the membranes, the glycerin has to be washed out (Supratec, 2020).

Most common packaging material is carton, but the fibers must be wrapped in plastic. Ideally the ends of the fibers should be attached together to keep the fibers straight and parallel (see Figure 19)



**Figure 19 - Professional packaging of hollow fiber membranes (MBR module).**

# 8  Product costs

## 8.1  Raw material costs

The costs of the raw materials needed for the production of 100 m$^2$ of hollow fibers plus 100 m$^2$ of flat sheet membranes are presented in Table 11. A factor of 20% is taken into account as wasted PVDF and NMP during the fabrication and cut-off of hollow fibers. The amount of polymer needed for the flat sheet membranes includes 22% extra material for non-effective areas. Since the solvent consumption of the flat sheet casting system is not known, the amount of NMP mentioned represents only the lab-scale system.

**Table 11 - Raw material costs**

| Raw material | Total amount needed for hollow fibers | Total amount needed for flat sheets | Price per unit | Total cost |
|---|---|---|---|---|
| PVDF | 13 kg (OD=1 mm) 26 kg (OD=2 mm) | 10 kg | 16-21 EUR / kg | 370-760 EUR |
| NMP | 66 kg (OD=1 mm) 130 kg (OD=2 mm) | 43 kg | 2-4 EUR / kg (industrial grade) 67 EUR / kg (analytical grade) | 220-700 EUR |

## 8.2  Labour costs

The labour costs for all production methods mentioned are presented in Table 12. Person months of 143 h are considered. For flat sheet production at pilot scale, it is assumed that preparation and cleaning last 1.5 h every day. For the semi-continuous methods, the hours mentioned do not include the time that the hollow fibers and flat sheet rolls spend in the washing bath and the drying time because these do not require labour. Potential defects and technical issues are not taken into account in these calculations.

**Table 12 - Labour costs**

| Product | Production scale | Hours | Persons needed | Equivalent Person months |
|---|---|---|---|---|
| Hollow fibers | Lab | 480 | 2 | 6.8 |
| | Pilot (OD=1 mm) | 350 | 1 | 2.5 |
| | Pilot (OD=2 mm) | 280-350 | 1 | 2.0-2.5 |
| Flat sheets | Lab | 5000 | 1 | 35 |
| | Pilot | 5-29 | 1 | 0.04-0.2 |

## 8.3  Benchmarking

Although it is not easy to find commercial membranes for MD with the required specifications, some examples are presented below:

Commercial-grade PVDF hollow fiber membranes of 0.7 mm inside diameter, 1.4 outer diameter and less than 0.1 µm pore size are sold for 900 USD  every 52 m$^2$ (approx. 1,480 EUR / 100 m$^2$) (Suntar Environmental Technology Pte Ltd., Singapore). Membrane modules with follow fiber dimensions of 0.6 mm inside diameter, 1.2 outer diameter and less than 0.1 µm pore size, are priced 698 USD for 55 m$^2$ (approx. 1,080 EUR / 100 m$^2$) (Hinada Water Treatment Tech Co., Ltd., China). Hollow fibers for with 0.7 mm inside diameter, 1.3 outer diameter and less than 0.05µm pore size are priced 150 USD for 10 m$^2$ (approx. 1,280 EUR / 100 m$^2$) (Guangzhou Vocee Membrane Technology Co.,Ltd., China).

Flat sheet membranes are usually produced industrially with a regular width shorter than the required 40 cm. Customised flat sheets of 40 x 70 cm are not common to find. The regular widths fabricated are 25, 32 and 42 cm. The quotation for customised 40 cm – wide hydrophobic PVDF flat sheet membranes of pore size of 1 μm is 1,900 USD (approx. 1,600 EUR) for 100 m$^2$, 3,746 USD (approx. 3,200 EUR) for 200 m$^2$ and 8,730 USD (approx. 7,400 EUR) for 500 m$^2$ (JiAn City Qing Feng Filter Equipment Material Co., Ltd., China).

## 8.4  Long-term footprint

The average greenhouse gas emission intensity (in $CO_2$ equivalent – $CO_2e$) for electricity generation in the European Union (27 countries, value of 2019) is around 255 g $CO_2e$/kWh (EEA, 2021). Greenhouse gas emission intensity (g $CO_2e$/kWh) is calculated as the ratio of $CO_2$ emissions from public electricity production (as a share of $CO_2$ equivalent emissions from public electricity and heat production related to electricity production), and gross electricity production.

The power consumption of the hollow fiber membrane production apparatus can be calculated as the sum of all power consuming parts. The Julabo MW-4 circulator for temperature control has a total power consumption of 2.15 kW, the two Mahr gear metering pump have a consumption of 2 x 0.25 kW and the KIMO MotorMaster MM1.5FMC-emc frequency inverters have a power of 2 x 1.5 kW. Together with the motor, the total power consumption is around 6 kW for both lab-scale and pilot-scale. The hourly consumption is equal to 6 kWh. Therefore, the greenhouse gas emission footprint is approximately 1,530 g $CO_2e$/h. The water consumption of every hollow fiber membranes' batch is 110 L of water to initially fill the coagulation baths plus 240 L/h of water for the circulating coagulant flow.

The flat sheet production at lab scale does not involve any power consumption. The system power of the PHILOS semi continuous flat sheet membrane casting system presented above is 1.5 kW. The hourly consumption is equal to 1.5 kWh, therefore, the greenhouse gas emission footprint is approximately 383 g $CO_2e$/h. The water consumption for lab-scale production is 30 mL per 21 x 30 cm sheet, while the coagulation bath of the PHILOS system is around 130 L.

The above numbers of greenhouse gas emission footprint do not include the production and transport of raw materials or the energy footprint of water consumption.

## 9  Conclusions

In conclusion, the scale-up of membrane production from lab to pilot scale is technically feasible with a few modifications of the existing hollow fiber production apparatus.

Flat sheet membranes can be easily produces in large scale provided that a semi-continuous flat sheet casting system is acquired.

Further morphological and performance evaluation of the produced membranes with the new systems will take place within the course of the project and will guide the selection, modification and optimization of appropriate protocols for the preparation of these membranes.

Also, it was concluded that the commercially available ion exchange resins are well suited for the requirements of intelWATT processes.

# References

Abetz, V., Brinkmann, T., Sözbilir, M., 2021. Fabrication and function of polymer membranes. Chem. Teach. Int. 3, 141–154. https://doi.org/10.1515/cti-2020-0023

Athanasekou, C., Sapalidis, A., Katris, I., Savopoulou, E., Beltsios, K., Tsoufis, T., Kaltzoglou, A., Falaras, P., Bounos, G., Antoniou, M., Boutikos, P., Romanos, G.Em., 2019. Mixed Matrix PVDF/Graphene and Composite-Skin PVDF/Graphene Oxide Membranes Applied in Membrane Distillation. Polym. Eng. Sci. 59, E262–E278. https://doi.org/10.1002/pen.24930

Balis, E., Sapalidis, A., Pilatos, G., Kouvelos, E., Athanasekou, Ch., Veziri, C., Boutikos, P., Beltsios, K.G., Romanos, G., 2019. Enhancement of vapor flux and salt rejection efficiency induced by low cost-high purity MWCNTs in upscaled PVDF and PVDF-HFP hollow fiber modules for membrane distillation. Sep. Purif. Technol. 224, 163–179. https://doi.org/10.1016/j.seppur.2019.04.067

Burgal, J. da S., Peeva, L., Livingston, A., 2016. Towards improved membrane production: using low-toxicity solvents for the preparation of PEEK nanofiltration membranes. Green Chem. 18, 2374–2384. https://doi.org/10.1039/C5GC02546J

Dallas, A.J., Ding, L., Joriman, J., Hoang, B., Seguin, K., Zastera, D., 2006. An investigation of the removal of 1-Methyl-2-Pyrrolidinone (NMP), in: Metrology, Inspection, and Process Control for Microlithography XX. Presented at the Metrology, Inspection, and Process Control for Microlithography XX, SPIE, pp. 1219–1235. https://doi.org/10.1117/12.654839

Drying of water treatment membranes, Filtration + Separation, Volume 55, Issue 3, 2018, Pages 22-27, ISSN 0015-1882, https://doi.org/10.1016/S0015-1882(18)30254-4.

European Commission, 2020. Critical Raw Materials Resilience: Charting a Path towards greater Security and Sustainability. 3. https://eur-lex.europa.eu/legal-content/EN/TXT/PDF/?uri=CELEX:52020DC0474&from=EN

EEA (European Environment Agency), 2021. Greenhouse gas emission intensity of electricity generation [WWW document]. URL https://www.eea.europa.eu/data-and-maps/daviz/co2-emission-intensity-8 (accessed 9.24.21).

Emergen Research, 2021. Polyvinylidene Fluoride Market Size - PVDF Market Report by 2028 [WWW Document]. URL https://www.emergenresearch.com/industry-report/polyvinylidene-fluoride-market (accessed 9.29.21).

Eykens, L., De Sitter, K., Dotremont, C., Pinoy, L., Van der Bruggen, B., 2017. Membrane synthesis for membrane distillation: A review. Sep. Purif. Technol. 182, 36–51. https://doi.org/10.1016/j.seppur.2017.03.035

Marshall, J.E., Zhenova, A., Roberts, S., Petchey, T., Zhu, P., Dancer, C.E.J., McElroy, C.R., Kendrick, E., Goodship, V., 2021. On the Solubility and Stability of Polyvinylidene Fluoride. Polymers 13, 1354. https://doi.org/10.3390/polym13091354

Miyata, K., Kawada, T., Katou, K., 2012. NMP distilling apparatus. EP2479167A1.

Ong, C.S., Lau, W.J., Al-anzi, B., Ismail, A.F., 2017. Photodegradation stability study of PVDF- and PEI-based membranes for oily wastewater treatment process. Membr. Water Treat. 8, 211–223. http://dx.doi.org/10.12989/mwt.2017.8.3.211

Öztürk, Y., Ekmekçi, Z., 2020. Removal of sulfate ions from process water by ion exchange resins. Minerals Engineering 159, 106613. https://doi.org/10.1016/j.mineng.2020.106613

Ren, Y., Li, X., Wu, J. (任月萍, 李秀芬, 吴杰), 2014. Recycling method of waste polyvinylidene fluoride (PVDF) flat sheet membrane. CN103752190A.

Supratec Membrane GmbH, Polyvinylidene Fluoride (PVDF) Ultrafiltration Membrane, Data Sheet, 2020, https://supratec-membrane.de/wp-content/uploads/2020/05/Supratec-Membrane_Data-Sheet-30nm-PVDF-UF-Membrane-April-2020.pdf

Tozzi, P.V., Wisniewski, C.M., Zalewski, N.J., Savelski, M.J., Slater, C.S., Richetti, F.A., 2018. Life cycle assessment of solvent extraction as a low-energy alternative to distillation for recovery of N-methyl-2-pyrrolidone from process waste. Green Process. Synth. 7, 277–286. https://doi.org/10.1515/gps-2017-0030

US EPA, O., 2019. Final Risk Evaluation for n-Methylpyrrolidone (NMP) [WWW Document]. URL https://www.epa.gov/assessing-and-managing-chemicals-under-tsca/final-risk-evaluation-n-methylpyrrolidone-nmp (accessed 9.22.21).

Wang, X., Xiao, C., Liu, H., Huang, Q., Chen, M., 2017. Fabrication and properties of recycled poly(vinylidene fluoride) (PVDF) hollow fiber membranes. Desalin. Water Treat. 87, 82–90. https://doi.org/10.5004/dwt.2017.21287

Yalçin, S., Apak, R., Hizal, J., Afşar, H., 2001. Recovery of Copper (II) and Chromium (III, VI) from Electroplating-Industry Wastewater by Ion Exchange. Separation Science and Technology 36, 2181–2196. https://doi.org/10.1081/SS-100105912

Zhao, K., Heinzl, W., Wenzel, M., Büttner, S., Bollen, F., Lange, G., Heinzl, S., Sarda, N., 2013. Experimental study of the memsys vacuum-multi-effect-membrane-distillation (V-MEMD) module. Desalination, Membrane Distillation and related Membrane Systems 323, 150–160. https://doi.org/10.1016/j.desal.2012.12.003

# Annex I – Properties of known solvents for PVDF

Table 13 - The properties of known solvents for PVDF (Marshall et al., 2021). All measurements are at 25 °C and 760 mmHg, unless noted otherwise. $\delta_D$, $\delta_P$, $\delta_H$ = Hansen solubility parameters, MP = melting point, BP = boiling point, FP = flash point, $\rho$ = density, $\eta$ = dynamic viscosity, and $\gamma$ = surface tension.

| Solvent | Green solvent | $\delta_D$ | $\delta_P$ | $\delta_H$ | MP | BP | FP | $\rho$ | $\eta$ | $\gamma$ |
|---|---|---|---|---|---|---|---|---|---|---|
| | | MPa$^{0.5}$ | | | °C | | | g/cm$^3$ | mPA • s | mN/m |
| Acetone | ✅ | 15.5 | 10.4 | 7.0 | -95 | 56 | -17 | 0.79 | 0.3 | 23.5 |
| Acetyl triethyl citrate (ATEC) | | 16.6 | 3.5 | 8.6 | -45 | 228[a] | 188 | 1.14 | 53.7 | |
| γ–Butyrolactone (GBL) | ✅ | 19.0 | 16.6 | 7.4 | -45 | 204 | 98 | 1.12 | 2.0 | 44.6 |
| Cyclohexanone (CHO) | | 17.8 | 6.3 | 5.1 | -31 | 154 | 44 | 0.95 | 2.2 | 35.1 |
| Cyclopentanone (CPO) | ✅ | 17.9 | 11.9 | 5.2 | -51 | 131 | 30 | 0.94 | 1.1 | 33.8 |
| Dibutyl phthalate (DBP) | | 17.8 | 8.6 | 4.1 | -35 | 339 | 171 | 1.05 | 19.7 | 33.4 |
| Dibutyl sebacate (DBS) | | 13.9 | 4.5 | 4.1 | -10 | 345 | 178 | 0.94 | 8.0 | 33.1 |
| Diethyl carbonate (DEC) | ✅ | 16.6 | 3.1 | 6.1 | -43 | 126 | 25 | 0.98 | 0.8 | 26.8 |
| Diethyl phthalate (DEP) | | 17.6 | 9.6 | 4.5 | -60 | 297 | 170 | 1.12 | 12.9 | 23.5 |
| Dihydrolevoglucosenone (Cyrene) | ✅ | 18.8 | 10.6 | 6.9 | -20 | 227 | 108 | 1.25 | 14.5 | 72.5 |
| Dimethylacetamide (DMAc) | | 16.8 | 11.5 | 10.2 | -20 | 166 | 64 | 0.94 | 0.9 | 32.4 |
| N,N–dimethylformamide (DMF) | | 17.4 | 16.7 | 11.3 | -61 | 153 | 58 | 0.94 | 0.9 | 35.2 |
| Dimethylsulfoxide (DMSO) | ✅ | 18.4 | 16.4 | 10.2 | 19 | 189 | 87 | 1.10 | 1.9 | 42.7 |
| 1,4–Dioxane | | 19.0 | 1.8 | 7.4 | 12 | 101 | 11 | 1.03 | 1.3 | 32.7 |
| 3–Heptanone | | 16.2 | 5.0 | 4.1 | -39 | 146 | 41 | 0.81 | 0.8 | 25.7 |
| Hexamethyl phosphoramide (HMPA) | | 18.5 | 8.6 | 11.3 | 7 | 231[b] | 144 | 1.03 | 3.5 | 34.4 |
| 3–Hexanone | | 15.7 | 6.7 | 4.1 | | -56 | 124 | 18 | 0.82 | |
| Methyl ethyl ketone (MEK) | | 16.0 | 9.0 | 5.1 | -86 | 80 | -9 | 0.81 | 0.4 | 24.3 |
| N–methyl–2–pyrrolidinone (NMP) | | 18.0 | 12.3 | 7.2 | -24 | 204 | 91 | 1.03 | 1.7 | 40.3 |
| 3–Octanone | | 16.2 | 4.5 | 4.1 | -23 | 169 | 53 | 0.82 | | 26.2 |
| Rhodiasolv® PolarClean | ✅ | 17.2 | 8.6 | 9.7 | -60 | 278 | 144 | 1.04 | 7.4 | 37.5 |
| 3–Pentanone | | 15.8 | 7.6 | 4.7 | -39 | 100 | 13 | 0.81 | 0.4 | 24.7 |
| Propylene carbonate (PC) | ✅ | 20.0 | 18.0 | 4.1 | -49 | 242 | 116 | 1.20 | 2.8 | 31.9 |
| Tetrahydrofuran (THF) | | 16.8 | 5.7 | 8.0 | -108 | 65 | -21 | 0.88 | 0.5 | 27.1 |

| | | | | | | | | | | |
|---|---|---|---|---|---|---|---|---|---|---|
| **Tetramethylurea (TMU)** | | 16.7 | 8.2 | 11.1 | -1 | 177 | 75 | 0.97 | 1.4 | 34.6 |
| **Triacetin** | ✅ | 16.5 | 4.5 | 9.1 | -78 | 258 | 148 | 1.16 | 22.5 | 35.2 |
| **Triethyl citrate (TEC)** | | 16.5 | 4.9 | 12.0 | -40 | 287 | 178 | 1.14 | 32.2 | 41.5 |
| **Triethyl phosphate (TEP)** | ✅ | 16.7 | 11.4 | 9.2 | -56 | 216 | 115 | 1.07 | 1.8 | 29.6 |
| **Trimethyl phosphate (TMP)** | | 16.7 | 15.9 | 10.2 | -46 | 197 | 107 | 1.20 | 2.3 | 37.0 |
| **N,N' tetrabutylsuccindiamide (TBSA)** | ✅ | 17.2 | 9.0 | 2.9 | -76 | >250 | | 0.96 | | |

[a] Measured at 100 mmHg and [b] measured at 740 mmHg.